

Structure of an *n*-butane monolayer adsorbed on magnesium oxide (100)T. Arnold,¹ S. Chanaa,² S. M. Clarke,³ R. E. Cook,² and J. Z. Larese^{1,2}¹*Oak Ridge National Laboratory, P.O. Box 2008, Oak Ridge, Tennessee 37831, USA*²*Department of Chemistry, Buehler Hall, University of Tennessee, Knoxville, Tennessee 37996, USA*³*BP Institute and Department of Chemistry, University of Cambridge, Cambridge, United Kingdom*

(Received 12 April 2006; published 31 August 2006)

Neutron diffraction has been used to characterize the structure of the solid phase of the completed monolayer of *n* butane on the MgO(100) surface at low temperature. The monolayer is found to adopt a commensurate ($7\sqrt{2} \times \sqrt{2}R45^\circ$) structure with lattice constants $a=29.47$ Å and $b=4.21$ Å, P_{2gg} symmetry and four molecules in the unit cell. Excellent agreement with the experimental diffraction pattern is realized, using a Lorentzian profile to describe the line shape.

DOI: [10.1103/PhysRevB.74.085421](https://doi.org/10.1103/PhysRevB.74.085421)

PACS number(s): 61.12.-q, 68.43.-h, 68.47.Gh, 61.46.Df

I. INTRODUCTION

Neutron scattering techniques are widely used to simultaneously probe the microscopic spatial and temporal behavior of condensed matter. While not typically a surface-sensitive probe, neutrons can also be applied to investigate the properties of molecules adsorbed on the surface of, or entrained within, high surface-to-volume ratio materials. Exfoliated graphite (with trade names Grafoil and Papyx) is one such material that has been extensively used in neutron-scattering studies of adsorption where the objective has been to determine the structure of simple molecules adsorbed on the graphite basal plane. These studies are possible because this form of graphite has surfaces that are easily prepared and kept clean, has a high specific area (>10 m² g⁻¹), and uniform (crystalline) surface exposure. Only a small number of other materials fulfill all of these requirements; consequently, a more limited understanding of molecular adsorption on nongraphitic materials exists. There is currently a surge of activity surrounding the synthesis and characterization of nanometer-scale materials. Metal oxides (MO) play an important role in this emerging nanotechnology field because they are used in a wide range of applications, such as in pigments for paints, supports for catalysts, base components in cosmetics and medical ointments and creams, and in optoelectronics, e.g., tunable and Micro Electro Mechanical Systems (MEMS) devices, actuators, and novel sensors/detectors. Despite this enormous growth in interest, open questions still remain for even the simplest of metal oxides (MO), like magnesium oxide (MgO), on how the surface corrugation, symmetry, and imperfections (vacancies and defects) affect the physical properties of the adsorbed molecular layer. The knowledge base is even less complete on the role MO surfaces play in mediating simple chemical reactions. By using a new synthetic process, large quantities of uniform, high-quality powders of MgO in the form of nanocubes with principally (100) exposure can be produced that are ideal for use in surface adsorption research. This material is currently being used as part of a comprehensive investigation of the adsorption properties of short-chain normal alkanes adsorbed on the MgO(100) surface using a combination of thermodynamic and neutron-scattering techniques. We report here recent neutron diffraction mea-

surements from adsorbed monolayers of deuterated *n* butane (C_4D_{10}) on the MgO(100) surfaces. To date there are published structures for the first two members of the alkane series (methane and ethane) thin films adsorbed on MgO(100).¹⁻⁴

II. EXPERIMENTAL DETAILS**A. Sample preparation**

The synthesis and subsequent handling of the MgO samples used in this study have been described in our earlier papers.^{5,6} Approximately 10 g of MgO powder (consisting of ~ 200 nm cubic particles with (100) surface exposure) were loaded into a thin-walled, cylindrical aluminum cell (25 mm diameter, 50 mm tall) in an argon-filled glove box and sealed using an indium wire o-ring. The cell was mounted on a cryogenic transfer stick specifically designed for use in neutron-scattering experiments. A compact, computer-controlled, gas handling system designed for use at neutron facilities was used to prepare the butane films (this device and related gas handling procedures have been described elsewhere).⁷ During a typical neutron experiment, butane gas is introduced into the sample cell at 190 K in aliquots of about one-tenth layer until the desired quantity of gas is adsorbed. The adsorbed film is then cooled at a rate of ~ 1 K/min to 140 K and then annealed there for several hours. Finally, the sample is slowly cooled (~ 0.5 K/min) to 4 K where the neutron diffraction measurements are performed.

B. Neutron diffraction

The neutron diffraction experiments were primarily performed at ISIS the pulsed spallation neutron source at the Rutherford Appleton Laboratory (Didcot, UK) using OSIRIS, a time of flight (TOF) instrument operating in the high-resolution, backscattering diffraction mode. The wavelength-defining choppers were typically run at a frequency of 25 Hz, producing a selectable, 4 Å wide wavelength band at the sample position. Collecting TOF diffraction data at several settings of the wavelength-band choppers and then “stitching” together the individual segments produces a single diffraction pattern. The OSIRIS instrument

sits at the end of a supermirror guide that views a liquid hydrogen moderator resulting in a high flux of thermal neutrons at the sample position from 2 to 8 Å. The combination of high-flux and well matched resolution ($\Delta d/d < 6 \times 10^{-3}$) available in the diffraction mode on OSIRIS makes it ideally suited for the study of adsorbed layers of small molecules.^{8–10} These neutron diffraction studies were performed using a difference technique in which the diffraction signal from the adsorbed monolayer film on the MgO surface is obtained by subtracting off the signal due to neutrons scattered by the bare MgO substrate and sample can before the butane film is adsorbed. A more limited set of complementary, low Q (large d spacing) diffraction data ($Q < 0.8 \text{ \AA}^{-1}$) was also recorded on the high-intensity diffractometer D20 at Institute Laue Langevin in Grenoble, France. The data obtained from D20 complements that obtained on OSIRIS because measurements covering a Q range not practically accessible on OSIRIS can be performed. The D20 diffraction studies were extremely important because we were able to establish that no (additional) low Q diffraction peaks (large d -spacing structures) were missed during our OSIRIS experiments.

III. RESULTS

A. Adsorption isotherms

As noted above, a systematic and comprehensive study of the adsorption properties of the alkanes on MgO is ongoing. Although the investigation of the adsorption thermodynamics of butane on MgO(100) surfaces using high-resolution volumetric adsorption isotherms is not completed, the preliminary findings were an extremely valuable guide for the neutron scattering investigations. A subset of isotherms between 158 K $< T <$ 182 K are shown in Fig. 1, while the inset illustrates the comparison of a butane isotherm (at 198 K) to a methane isotherm (77 K) performed on the same MgO sample. Previous thermodynamic and structural studies of methane adsorbed on MgO(100) powders have established that the first layer forms a commensurate $\sqrt{2} \times \sqrt{2}R45^\circ$ solid phase with a surface area per molecule (APM) of 17 \AA^2 at temperatures below $\sim 80 \text{ K}$.^{3,6} Using this value and comparing the relative number of molecules needed to complete the first layer for methane and butane isotherms (on the same MgO sample), we have determined that the APM of butane is 42 \AA^2 (at 180 K). This 42 \AA^2 should be an upper bound for the APM of the monolayer butane solid phase at low temperature. The lower bound for the APM of the monolayer solid can be set at $\sim 30 \text{ \AA}^2$ by noting the minimum two-dimensional (2D) “footprint” of butane molecules lying with their long axis parallel to the surface of the substrate based on the molecular dimensions determined from structural studies of the bulk butane crystal structure.¹⁰ Furthermore, an APM of 33 \AA^2 was found for monolayer butane film adsorbed on graphite.¹¹ By combining the thermodynamic and structural information above with simple steric models of n -butane molecules a trial structure that placed the butane molecules on the MgO(100) surface with the long axis parallel to the surface was chosen as a starting point for analyz-

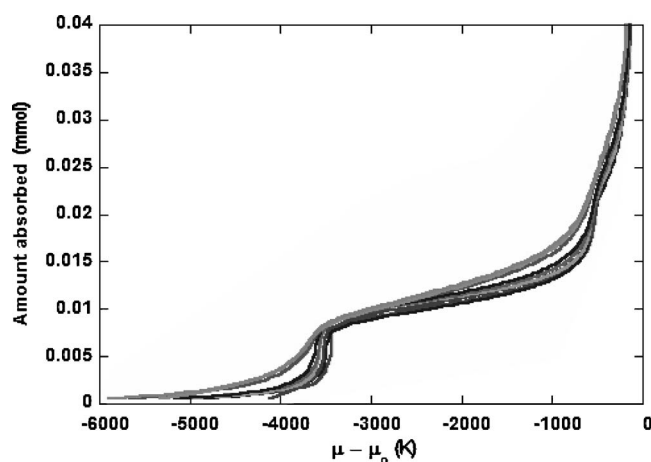


FIG. 1. Butane isotherms in the temperature range 158–182 K. The inset compares an isotherm from methane and one from butane measured on the same sample to estimate the surface area of each butane molecule. It is clear that two layering transitions are evident. This behavior is similar to that observed for propane and ethane on MgO, whereas methane forms at least seven discrete layering transitions. The butane surface coverage used in the diffraction measurements corresponds to the crest of the first step of the isotherm, equivalent to $\sim 0.08 \text{ mmol}$, or “monolayer completion.”

ing the neutron diffraction data described below.

B. Diffraction results and structural analysis

A typical neutron diffraction pattern from a solid monolayer butane film adsorbed on MgO(100) at 4.2 K is shown in Fig. 2. The diffraction data shown in Fig. 2 are of remarkably good quality (when compared with data previously published in other adsorbed film studies). The pattern consists of seven distinct diffraction peaks, each with the characteristic “Warren” (i.e., sawtooth) line-shape^{12–14} representative of the scattering from a randomly oriented, 2D, crystalline solid with long-range order. The positions of all the observed

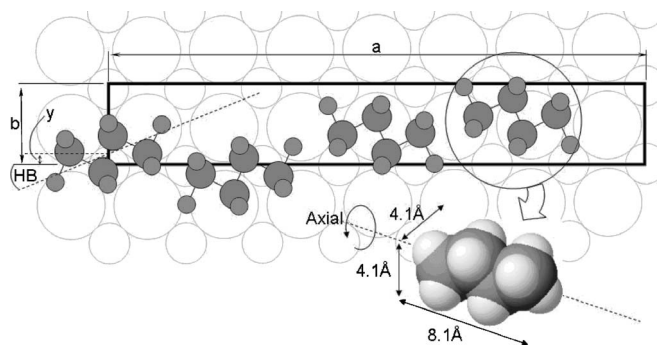


FIG. 2. Schematic picture of the P_{2gg} structure adopted by n butane on MgO, which illustrates the molecular arrangement and defines the fit parameters; a and b are the unit cell parameters, HB is the “herringbone” angle, and y is the displacement along the b axis. The centers of the four molecules within the unit cell are thus located at $(0, +y)$, $(\frac{a}{4}, -y)$, $[\frac{a}{2}, (\frac{b}{2} - y)]$, and $[\frac{3a}{4}, (\frac{b}{2} + y)]$. The positions of the atoms are then defined by the coordinates listed in Table II with the HB and axial rotations applied.

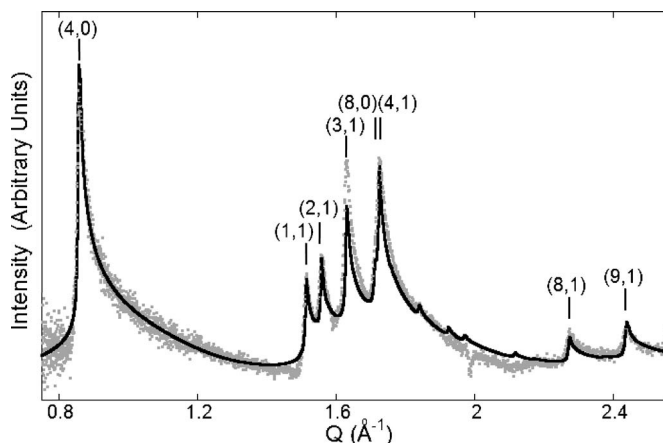


FIG. 3. Experimental diffraction pattern and “best-fit” calculated pattern for *n* butane adsorbed on MgO. The peaks are indexed for the rectangular unit cell $a=29.47$ Å, $b=4.21$ Å.

peaks, including the weak peak (indexed as (5,1) in Fig. 3), are listed in Table I. While the diffraction data tabulated there is from the ISIS experiments, it is consistent with data collected on D20 (not shown). As noted above, the D20 experiments did not yield any evidence of additional diffraction peaks at low Q . The same procedure used to previously analyze the neutron diffraction data was followed here.^{3,15–17} It is often a challenge to determine the structure in these adsorbed film studies because the accuracy of the structural parameters is directly tied to the number of diffraction peaks observed. In order to simplify the determination of the butane on MgO film structure, we limited the number of free parameters. For example, the intramolecular bond lengths and angles were set to those determined through optimization of a free gas molecule using Gaussian.¹⁸ Furthermore, the initial unit cell dimensions and the molecular orientations used the steric models and APM considerations noted above as a guide during our structural determination. Using these conditions, we quickly found that a rectangular unit cell with lattice constants $a=29.47$ Å and $b=4.21$ Å and containing four butane molecules, adheres to the close-packing conditions described by Kitaigorodskii¹⁹ and accounts for all the diffraction peaks we recorded. Using these cell parameters, one calculates an area occupied by each molecule of 31 Å², a value that compares favorably with the considerations above. After several additional trials, we found that when the molecules are arranged in a 2D structure with P_{2gg} symmetry

TABLE I. A comparison of the experimental and calculated peak positions. The positions of the peaks are given in momentum transfer, Q (Å⁻¹).

Observed	Position	Index
0.851 ± 0.007	0.8528	(4,0)
Not observed	1.2792 (negligible intensity)	(6,0)
1.510 ± 0.005	1.5076	(1,1)
1.550 ± 0.005	1.5522	(2,1)
1.622 ± 0.005	1.6237	(3,1)
1.720 ± 0.005	1.7056	(8,0)
	1.7189	(4,1)
1.84 ± 0.02 (low intensity)	1.8341	(5,1)
Not observed	1.9657 (negligible intensity)	(6,1)
Not observed	2.1106 (negligible intensity)	(7,1)
2.267 ± 0.005	2.2664	(8,1)
2.430 ± 0.005	2.4309	(9,1)

yielded the very best fit to the experimental data. We note that this arrangement produces systematic absences of diffraction peaks with Miller indices $(h,0)$ with h =odd and $(0,k)$ with k =odd. Centered unit cells with higher symmetry did not produce systematic absences consistent with our experimental diffraction data. By keeping the intramolecular bond lengths and angles of the molecule fixed, the only adjustable parameters needed to calculate the diffraction profile is the “herringbone” (HB) and “axial” (AX) angles and the relative displacement along the b direction (y) (see Fig. 2 and Ref. 16). The final values used to obtain the calculated pattern (Fig. 3) are given in Table II. This represents the best-fit to the experimentally observed diffracted intensities. The sensitivity of the calculated intensities to the values of HB, AX, and y their error limits. We note that the AX values quoted in Table II are for rotations of each pair of molecules in the unit cell. The two molecules closest to the origin form one “pair” of molecules while the remaining two form the second pair. All rotations are with respect to the “starting positions” given by the Cartesian coordinates provided in Table II. We note that the significant enhancement in the signal-to-noise ratio realized by performing these measurements with OSIRIS yields a significant advantage (and challenge) when a calculation of the line shape of the entire diffraction pattern is attempted. While it is obvious from an inspection of the diffraction data that they have a sawtooth

TABLE II. Fit Parameters.

Atom	x	y	z	Fit parameters	
C1	-1.9336	-0.1281	0.0000	$a/\text{Å}$	29.47 ± 0.25
C2	-0.5470	0.5420	0.0000	$b/\text{Å}$	4.21 ± 0.02
D1 and D2	-2.0352	-0.7374	0.8737	$V/^\circ$	90
D3 and D4	-0.4453	1.1513	0.8737	HB angle/ $^\circ$	18 ± 1
D5	-2.6936	0.6250	0.0000	y (displacement)/Å	0.37 ± 0.05
				AX angle (pair 1)/ $^\circ$	35 ± 25
				AX angle (pair 2)/ $^\circ$	55 ± 25

appearance, even a cursory attempt at fitting the entire diffraction pattern makes it clear that Warren's description of the 2D line shape will not reproduce the experimental diffraction pattern well. This requires us to consider some other methods for describing the functional form of the line shape. Fortunately, the literature contains several alternative 2D line profile descriptions to Warren's approach, including one based on strain-induced defect formation,¹⁹ and others where a Lorentzian or Lorentzian-squared decay of the scattering intensity occurs as one moves away from the Bragg position of the actual rods.²⁰ In this study, we found that a Lorentzian profile gives the best fit to the data.

In addition to the parameters that determine the size of the unit cell and the location/orientation of the molecules within the cell and the functional form of the diffraction profile, several other factors must be considered to calculate the diffraction profile. The spatial correlation length was set to ~ 300 nm, a value consistent with the size of the MgO nanocubes. The Debye-Waller factor was set to unity because these experiments were performed at 4 K where the thermal motion was considered to be negligible. No correction was used (or needed) to account for the preferential ordering of the MgO powder (unlike diffraction studies of alkanes adsorbed oriented graphite substrates like Grafoil or Papyex). This is consistent with earlier studies of methane on MgO(100) and suggests that the samples can be considered randomly oriented powders. The resolution function for the instrument was obtained using the OSIRIS calibration data and the convolution parameters described in the General Structure Analysis System (GSAS) manual.

IV. DISCUSSION

Inspection of Fig. 3 clearly indicates that the calculated line shapes, using the parameters and considerations discussed above, reproduces the neutron diffraction pattern remarkably well and reaffirms that our structural assignment is good. The best fit to the experimental data (detailed in Table II) actually deviates slightly from true P_{2gg} symmetry. This finding is probably the result of the restrictions we placed on rigidity of the intramolecular bond lengths and angles used in the fit and also because we believe a small amount of orientational disorder is most likely present. We note, however, that the calculated line-shape structure is rather sensitive to the choice of HB angle. There is a significant amount of confidence to be placed in the HB angular assignment and resulting error (we estimate that the value quoted for HB is not off by more than 1° from the reported value).

A. Comparison with adsorption on graphite and bulk structure

It has been shown that several of the n alkanes, e.g., ethane, hexane, and octane, also form commensurate, rectangular monolayer solid structures on the basal plane of graphite with the molecules arranged in a herringbone pattern with P_{2gg} symmetry.¹⁶ The formation of a commensurate overlayer usually indicates that the corrugation of the underlying potential energy surface reinforces the stability of the solid film. On graphite, it has been proposed that the excellent

match of the alkane's C-C backbone to the hexagonal graphite surface net is responsible for aiding the commensurability.²¹ For butane on graphite, the literature^{11,22-26} indicates that a commensurate structure forms that closely resembles the (100) plane of the bulk butane crystal. It is worth considering whether the butane-on-MgO structure bears any simple relationship to the bulk solid structure. The results we presented above indicated that the best fit was found with unit cell parameters $a=29.47$ Å and $b=4.21$ Å. These values that strongly suggest that the butane monolayer film forms a $7\sqrt{2} \times \sqrt{2}R45^\circ$ commensurate solid with the underlying MgO(100) surface (lattice parameter, 2.98 Å). Unlike the graphite case, however, no simple relationship exists between the commensurate film structure we deduced from our fitting procedure and a low index plane of the bulk crystal. During our structural analysis, trial structures with unit-cell dimensions and molecular distributions close to the low index bulk planes were considered,¹⁰ but these did not yield diffraction patterns that were close to our experimental pattern. Finally, we can also use the results of our preliminary adsorption isotherms displayed in Fig. 1 to comment further on the possible structural relationship of the film to the bulk butane solid. Substrates well matched to the structure of a low index plane of the adsorbates bulk solid tend to show numerous layering steps (i.e., >4 or 5) in the adsorption isotherm. For example, previous adsorption studies of methane on MgO(100) revealed an adsorption isotherm with six or seven distinct steps and that the structure of bulk methane (II) (100) is a close match for the (100) face of the MgO. On the other hand, Fig. 1 shows that the adsorption isotherms for butane on MgO have only two steps even in the lowest temperature traces. Hence the absence of multilayer stepwise growth extending beyond two solid layers seems to also imply that no simple relationship exists between the film structure and one of the low index surfaces of the bulk solid.

V. CONCLUSION

We have used neutron diffraction to determine the structure of a solid monolayer film of deuterated n butane adsorbed on the MgO(100) surface at 4 K. The solid adopts a commensurate, $7\sqrt{2} \times \sqrt{2}R45^\circ$, herringbone structure with P_{2gg} symmetry and four molecules per unit cell. The excellent fit to the diffraction data lends confidence that these data can be used as dependable constraints for developing potential energy surfaces. The next steps in this investigation will be to complete a thorough thermodynamic investigation of the n -butane/MgO system, use the thermodynamic findings and the structural findings to perform accurate computer modeling of the minimum energy configuration of the molecules within the solid, and to develop an accurate potential energy surface. These results will then be used to predict and to understand the dynamical properties of the butane monolayer solid to be explored in a separate inelastic neutron-scattering investigation. Furthermore, the evolution of the butane film structure and dynamics with coverage and temperature, particularly in the bilayer region, should also be informative.

ACKNOWLEDGMENTS

The authors would like to thank Julius Hastings, Richard Ibberson, David Beach, John Tomkinson, and Bobby Sumpter for useful discussions and Mark Telling and Thomas Hansen for help at ISIS and the ILL, respectively. In addition we would like to thank Tim Free for producing the sample cells and the members of the ISIS user support of the

group for their assistance. This work was performed with the support of the Division of Materials Sciences, Office of Basic Energy Sciences, U.S. Department of Energy, under Contract No. DE-AC05-00OR22725 with Oak Ridge National Laboratory, managed and operated by UT-Battelle, LLC. UTK, ISIS, and BP Institute Cambridge provided J.Z.L. with supplementary support.

-
- ¹M. Trabelsi and J. P. Coulomb, *Surf. Sci.* **272**, 352 (1992)
²M. Sidoumou, T. Angot, and J. Suzanne, *Surf. Sci.* **272**, 347 (1992).
³J. Z. Larese, *Physica B* **248**, 297 (1998).
⁴J. Z. Larese, D. M. Y. Marero, D. S. Sivia, and C. J. Carlile, *Phys. Rev. Lett.* **87**, 206102 (2001).
⁵W. Kunmann and J. Z. Larese, Patent 6,179,897, U.S.A. (2001).
⁶A. Freitag and J. Z. Larese, *Phys. Rev. B* **62**, 8360 (2000).
⁷Z. Mursic, M. Y. M. Lee, D. E. Johnson, and J. Z. Larese, *Rev. Sci. Instrum.* **67**, 1886 (1996).
⁸M. A. Castro, S. M. Clarke, A. Inaba, R. K. Thomas, and T. Arnold, *J. Phys. Chem.* **105**, 8577 (2001).
⁹M. A. Castro, S. M. Clarke, A. Inaba, R. K. Thomas, and T. Arnold, *Phys. Chem. Chem. Phys.* **3**, 3774 (2001).
¹⁰M. A. Castro, S. M. Clarke, A. Inaba, T. Arnold, and R. K. Thomas, *Phys. Chem. Chem. Phys.* **1**, 5017 (1999).
¹¹K. Refson and G. S. Pawley, *Acta Crystallogr., Sect. B: Struct. Sci.* **42**, 402 (1986).
¹²K. W. Herwig, J. C. Newton, and H. Taub, *Phys. Rev. B* **50**, 15287 (1994).
¹³B. E. Warren, *Phys. Rev.* **59**, 693 (1941).
¹⁴A. J. C. Wilson, *Acta Crystallogr.* **2**, 245 (1949).
¹⁵B. E. Warren and P. Bodenstein, *Acta Crystallogr.* **20**, 602 (1966).
¹⁶T. Arnold, R. K. Thomas, M. A. Castro, S. M. Clarke, L. Messe, and A. Inaba, *Phys. Chem. Chem. Phys.* **4**, 345 (2002).
¹⁷T. Arnold, C. C. Dong, R. K. Thomas, M. A. Castro, A. Perdigon, S. M. Clarke, and A. Inaba, *Phys. Chem. Chem. Phys.* **4**, 3430 (2002).
¹⁸M. J. Frisch, G. W. Trucks, H. B. Schlegel, *GAUSSIAN 03, Revision C.02*, Gaussian, Inc., Wallingford, CT, 2004.
¹⁹A. I. Kitaigorodskii, *Molecular Crystals and Molecules* (Academic Press, New York, 1973).
²⁰S. Ergun and M. Berman, *Acta Crystallogr., Sect. A: Cryst. Phys., Diffr., Theor. Gen. Crystallogr.* **29**, 12 (1973).
²¹H. P. Schildberg and H. J. Lauter, *Surf. Sci.* **208**, 507 (1989).
²²A. J. Groszek, *Proc. R. Soc. London, Ser. A* **314**, 473 (1969).
²³G. J. Trott, H. Taub, F. Y. Hansen, and H. R. Danner, *Chin. Phys. Lasers* **78**, 504 (1981).
²⁴R. Wang, H. Taub, H. J. Lauter, J. P. Biberian, and J. Suzanne, *J. Chem. Phys.* **82**, 3465 (1985).
²⁵F. Y. Hansen and H. Taub, *Phys. Rev. B* **19**, 6542 (1979).
²⁶H. Taub, H. R. Danner, Y. P. Sharma, H. L. McMurry, and R. M. Brugger, *Phys. Rev. Lett.* **39**, 215 (1977).